

# Atomistic mechanisms of rf breakdown in high-gradient linacs

Z. Insepov\*, J. Norem,  
Argonne National Laboratory, Argonne, IL 60439, USA  
S. Veitzer,  
Tech-X, Boulder, CO 80303, USA.

## Abstract

Molecular dynamics (MD) models of sputtering solid and liquid surfaces - including the surfaces charged by interaction with plasma, Coulomb explosion, and Taylor cone formation - were developed. MD simulations of self-sputtering of a crystalline (100) copper surface by  $\text{Cu}^+$  ions in a wide range of ion energies (50 eV – 50 keV) were performed. In order to accommodate energetic ion impacts on a target, a computational model was developed that utilizes MD to simulate rapid atomic collisions in the central impact zone, and a finite-difference method to accommodate the energy and shock wave absorption for the collisional processes occurring at a longer time scales. The sputtering yield increases if the surface temperature rises and the surface melts as a result of heat from plasma. Electrostatic charging of the surface under bombardment with plasma ions is another mechanism that can dramatically increase the sputtering yield because it reduces the surface binding energy and the surface tension. An MD model of Taylor cone formation at a sharp tip placed in a high electric field was developed, and the model was used to simulate Taylor cone formation for the first time. Good agreement was obtained between the calculated Taylor cone angle ( $104.3^\circ$ ) and the experimental one ( $98.6^\circ$ ). A Coulomb explosion (CE) was proposed as the main surface failure mechanism triggering breakdown, and the dynamics of CE was studied by MD.

Keywords: Molecular dynamics, sputtering, solid, liquid, surface, Taylor cone, Coulomb explosion.

PACS codes : 68.49.Sf; 41.75.Ak; 79.77.+g; 79.90.+b

## 1. Introduction

Energetic ion collisions with solid targets are an important area of research in basic science [1-8], as well as in numerous industrial applications [9-16]. Tech-X Inc.<sup>1</sup> has been developing multiphysics finite-element packages, including TXphysics, OOPIC, and, most recently, VORPAL, that are capable of simulating the dynamics and interaction of metal plasma with the surfaces in various *rf* structures. As does any finite-element package, these computational tools need the plasma-surface interaction characteristics, such as the sticking, reflection, and sputtering coefficients, that ultimately define the atomic flux from the surface to the plasma (i.e., fueling the latter) as a boundary condition. Since the sticking and sputtering yield coefficients are the atomistic characteristics of the plasma ion interaction with the surface, they can be calculated directly by either Monte Carlo or molecular dynamics methods.

Self-sputtering processes are also of fundamental interest in the development of high-gradient *rf* accelerators [1]. At least three research and development efforts are independently studying the behavior of high-gradient *rf* structures for accelerators. The Neutrino Factory and Muon Collider Collaboration (NFMCC) is looking at developing low-frequency structures for muon

---

\* Corresponding author, [insepov@anl.gov](mailto:insepov@anl.gov), 9700 South Cass Ave, Argonne, IL 60561

<sup>1</sup> <http://www.txcorp.com>

cooling [2–6], the International Linear Collider is optimizing the performance of 1.3 GHz superconducting rf structures aimed at the design of a 1 TeV superconducting electron/positron collider [7], and the High Gradient RF Collaboration is studying high-frequency ( $f > 10$  GHz) structures aimed at an electron-positron collider operating at energies higher than 1 TeV [8].

Understanding self-sputtering is also important for cathode discharge applications such as surface coating and modification [9,10], explanation of the unipolar arc development [11,12], detection of fast ions and particles [13,14], formation of columnar defect in alloys for fast particle registration [15], integrated circuits development based on copper connectors, and thin-film deposition development [16,17].

Experimental studies of the self-sputtering were carried out in [16] and discussed in [17,18]. Sputtering yields of metal ion beams, with energies from 10 to 500 eV, on polycrystalline Au, Cu, Ag, Cr, and Al films were measured in situ by using crystal microbalance techniques. A momentum-transfer model was developed that predicts the sputtering yield in the form

$$Y = K \left( \frac{E}{\lambda} \right) \left[ \frac{m_1 m_2}{(m_1 + m_2)^2} \right], \quad (1)$$

where  $K$  is the coefficient depending on the material,  $E$  is the ion energy, and  $\lambda$  is the penetrations depth (range) of ion in the target ( $\lambda \approx 10 \text{ \AA}$  at 300 eV for all studied metals). Equation (1) was found to be applicable in both high-ion and low-ion energy ranges, with an accuracy of  $\sim 20\%$  [16].

Physical and ion-enhanced chemical etch yields by noble gas and metal ions were fitted by a square root function down to the threshold energy for self-sputtering of metals, noble gas sputtering of metals, Si, SiO<sub>2</sub>, and ion beam etching of Si in [17]. Energetic ion-surface collisions used in thin-film technology imply both favorable effects such as promoting epitaxial growth and deleterious effects, since such collisions can introduce structural and/or compositional defects in the film. Both processes depend on the ion energy; and, therefore, optimization of the growth processes by selecting ion energies for fabrication of high-quality thin films is a high demand. Analysis of ion collisions was, provided for a wide variety of projectile ion/target material at very low ion energies. A universal dependence was proposed that describe the etching rate for semiconducting, insulating and metal surfaces above the threshold energies.

The sputtering yield  $Y$ , which is the number of neutral atoms ejected per incoming ion, can be expressed according to Sigmund's theory as follows:

$$Y(E) = C_{pt} S_n \left( \frac{E}{E_{pt}} \right), \quad (2)$$

where  $C_{pt}$  and  $E_{pt}$  are constants that depend on the projectile ion  $p$  and target material  $t$ , and  $S_n(\epsilon)$ ,  $\epsilon = E/E_{pt}$ , is a universal function, the nuclear stopping cross-section, depending on the reduced energy  $\epsilon$ .  $C_{pt}$  can be expressed via the surface binding energy  $U$ , and  $S_n(\epsilon) \sim E^{1/2}$ , for  $\epsilon \leq 0.02$ . Steinbrüchel [17] proposed a formula based on a detailed comparison to experimental data:

$$Y(E) \approx A \left( E^{1/2} - E_{th}^{1/2} \right), \quad (3)$$

where  $A$  and  $E_{th}$  are constants of the incoming ion/target material.

As mentioned above, the sputtering yield is a boundary condition for finite-element plasma simulation codes and can be calculated by atomistic simulation methods, such as Monte Carlo or molecular dynamics. Monte Carlo (MC) is the main method for sputtering yield calculations and was developed in a series of papers [18-20]. A Monte Carlo code T-DYN was developed by Biersack et al. [19]. The standard MC code simulates the event of an ion collision with the virgin target, without defect accumulation in the target from ion impacts. This code was applied to various ion/target material combinations in [20,21].

A self-sustained self-sputtering occurring during high-current pseudospark operation ( $\approx 10^4$  A/cm<sup>2</sup>,  $I > 10^3$  A) is shown in [21] to be a possible mechanism for superdense glow. The mean-free-path for ionization of cathode material sputtered in the low-current hollow-cathode phase can be shorter than the cathode-anode gap distance, and ionized atoms can return to the cathode surface, self-sputtering with a yield greater than one. The self-sputtered cathode atoms become ionized in the beam of electrons accelerated in the cathode sheath. As was shown in [21], a large fraction of the discharge current at the cathode surface can be carried uniformly over the surface by ions, and a very high electron emission density is not required to maintain the high current.

A review of the method of MD computer simulation and results obtained for the physics of sputtering is given in [18]; the physical input (such as the interatomic potentials, coupling to the electronic system), reliability, and computer time requirements of simulations are discussed. MD results obtained after 1992, the time of the last review, are presented, with an emphasis on results that are difficult to obtain by other theoretical or computational means: sputtering from high-energy-density zones (spikes), cluster emission, formation of surface topography and their influence on sputtering, and chemical effects.

MD simulations of self-sputtering and sticking coefficients of low-energy ion were reported in [22]. Sputter yields  $Y$  and sticking coefficients  $S$  are essential inputs for evolution studies of feature profiles. MD simulations are used to compute sputter yields and sticking coefficients for Cu ions impinging on a Cu surface at various incident energies  $15 < E_i < 175$  eV and incident angles  $0 < \theta_i < 85^\circ$ . Threshold energies for sputtering  $E_{th}$  are also predicted and shown to vary with  $\theta_i$ . Abrams and Graves [22] showed that for energies below the experimental threshold for physical sputtering ( $E_{th(\text{expt})} \sim 60$  eV), a yield between 0.01 and 0.1 Cu/ion still can be obtained for some off-normal angles of incidence. A dependence  $Y \propto E_i - E_{th}$  was found to be valid below  $E_{th(\text{expt})}$  when  $Y$  is a maximum with respect to  $\theta_i$  (at  $\theta_i = 45^\circ$ ). It was also shown that a dependence  $Y \propto E_i^{1/2} - E_{th}^{1/2}$  is more suitable at other incidence angles [22].

MD simulations were also used to calculate scattering and penetration of normally incident hyper thermal ( $5 < E_i < 400$  eV) of Ne, Ar, and Xe atoms off a Cu crystal [23]. The authors showed that the incident energy was efficiently deposited in the solid and that the deposited fraction depends mostly on the projectile mass, and less on the bombarding energy. At low

energy, the larger part of the nondeposited energy is taken away by the reflected projectile. Above the sputter threshold, an amount between 2% and 6% of the incident energy was carried by the sputtered particles. The results compared well with experiment. Gades and Urbassek [23] demonstrated that a realistic interaction between the projectile and the target atoms influences the energy deposition at energies below around 100 eV.

Several researchers have used MD simulations to study Coulomb explosion events occurring at energetic heavy and highly charged ion collisions with solid targets [13,24,25].

One of the goals of the simulations we present here is to verify and benchmark the sputtering yields used as an input file in the Txphysics and OOPIC software packages developed at Tech-X Inc. We also describe a preliminary interface between Vorpil and MD that we have constructed based on the exchanges of input/output files from one simulation level to another.

## 2. Simulation Models

This section focuses on the sputtering and Coulomb explosion models developed for simulation studies.

### 2.1. Sputtering Model

The evolution of the atomic system was determined by the solution of the set of the classical equations of motions for all the atoms in the system. The copper target was represented by crystalline (100) copper substrates, with the sizes dependent on the ion kinetic energy. All substrates were prepared by equilibration at room and elevated temperatures. Additional simulations were used to prepare a liquid copper surface for self-sputtering simulations.

The energetic ions were placed at a certain distance  $z_i$  above the target's surface (see Fig. 1), where the distance to the surface  $z_i$  was varied in three Cartesian directions within approximately one lattice parameter in order to randomize the collision event for further averaging. The ions were directed toward the target at an impact angle of  $5^\circ$ , in order to prevent channeling mode. The ion energies were selected in an interval from 50 eV to 50 keV, in order to compare with the existing sputtering yield data.

The size of the target is critical for the correct calculation of the sputtering yield since the shock-waves resulting from impacts have a velocity of  $\sim 5$  km/s in copper and therefore are reflected from the basic cell's boundaries within 1-2 ps. If no special measures are taken to suppress or mitigate these waves, they can drastically change the calculated result. Therefore, a parallelepiped with the volume of  $20 \times 20 \times 30 a_0^3$  containing approximately 42,000 copper atoms was used for most of the simulations, where  $a_0$  is the lattice parameter of the copper face-centered cubic (fcc) basic cell at RT. The lattice parameter can always be adjusted to a desired simulation temperature  $T$ :

$$a(T) = a_0(1 + \alpha(T - 293K)), \quad (4)$$

where  $a_0$  is a lattice period at room temperature obtained from experiment and the theory (see, e.g., [28,29]) and  $\alpha$  is the linear expansion coefficient,  $\alpha = 1.66 \times 10^{-5} \text{ 1/K}^2$ . The lattice parameter change was necessary for our high-temperature simulations of sputtering and for simulation of Coulomb explosion. The latter usually occurs at a temperature close to the melting point of copper,  $T_m = 1310 \text{ K}$ .

Periodic boundary conditions at low and thermal boundaries at higher energies were used to fix the system in the horizontal position, and two bottom atomic layers of the target were fixed to remove the movement of the target in the vertical direction.

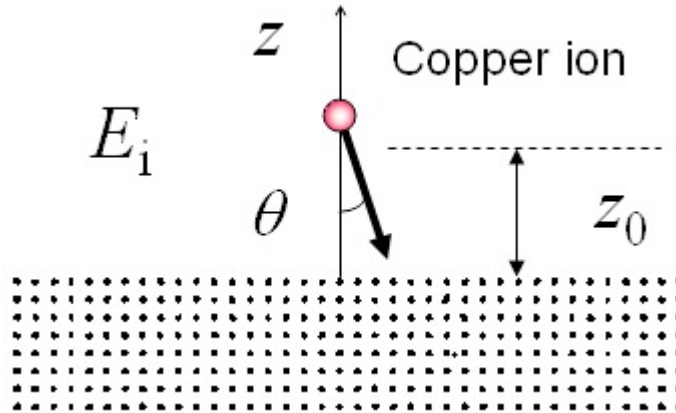
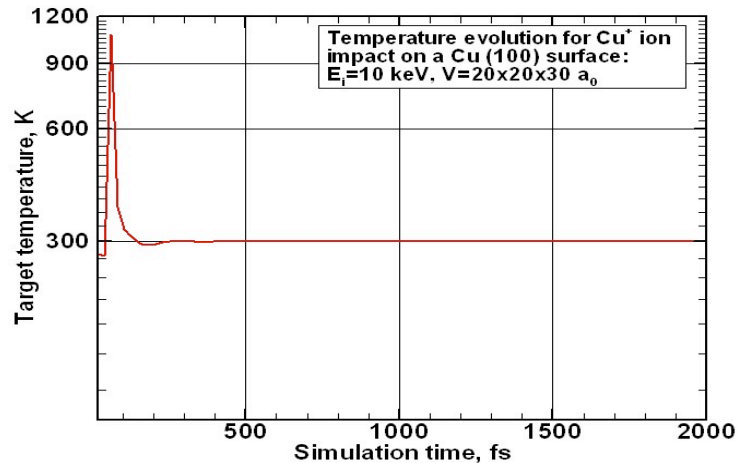


Fig. 1 Schematic of the target atoms (dots) and a copper ion (large circle) before the impact for sputtering simulation.  $\theta$  is the incoming angle of the ion,  $E_i$  is the ion energy, and  $z_0$  is the level above which the ejected target particle is assumed to be leaving the surface and counted as sputtered (see, e.g., [27] for more details)

Thermal boundaries were applied to the simulation system in order to remove the excess energy delivered by the energetic ion impact to the target's surface. This model was developed in our earlier papers [26,27] and is capable of completely removing the effect of shock waves and extending the simulation time for a single impact up to 20 ps (i.e., ten times longer than that of the conventional periodic boundary conditions, or PBCs).



<sup>2</sup> [http://www.engineeringtoolbox.com/linear-expansion-coefficients-d\\_95.html](http://www.engineeringtoolbox.com/linear-expansion-coefficients-d_95.html)

Fig. 2. Temperature evolution during the  $\text{Cu}^+$  ion impact on a copper target surface. The initial temperature  $T_s=300\text{K}$ . The energy released during the impact was absorbed by several thermal boundary layers.

Interactions between copper ions were modeled by using the embedded-atom method (EAM) many-body potentials derived from a second-moment approximation of the tight-binding quantum mechanics scheme in [28,29]. Two interatomic potential sets were used - Potential #1:  $E_c=3.5\text{ eV}$ ,  $Z_{nn}=12$ ,  $p=10.08$ ,  $q=2.56$ , where  $E_c$  is the cohesion energy,  $Z_{nn}$  is the number of nearest neighbors, and  $p$ ,  $q$  are the potential function exponents; and Potential #2:  $p=10.96$ ,  $q=2.278$ ,  $A=0.0855$ ,  $B=1.224$ . The radius of the potential cut was chosen to be between the first and second neighbors in both cases.

The self-sputtering yield  $Y$  (atoms/ion) was defined as the number of target atoms completely removed from the surface with one ion impact into vacuum. The atoms was considered as being removed if they reached a certain distance  $z_0$  above the surface where they had a kinetic energy of the momentum component in the vertical direction (normal to the surface) that was sufficient to overcome the attractive forces between the surface and the atom.

The sputtering yield calculation was based on a temporal evolution of the numbers of copper atoms ejected from the surface as a result of ion impact. The sputtering yield was calculated at different time instants from the beginning of the impact, and the calculation was continued until the yield became a constant, which was then used as a final yield value [27]. The longest MD run was calculated up to 20 ps of the MD time.

The time evolution of the total energy and evolution of the kinetic temperature of the target—an average kinetic energy of the target atoms per atom—were used as a benchmark test for the computer code. It is well known that the PBCs create an unphysical reflection of elastic waves and the so-called Rahman's echo; indeed, both can drastically alter the calculated yield. Our thermal boundaries were developed specifically to be able to remove reflection of shock waves from the system boundaries in our previous papers [26,27]. These boundaries can efficiently remove elastic waves and thermal energy from the basic cell by coupling the MD atomistic system to a continuum elastic media described by elasticity and thermal diffusion equations. Figure 2 shows a 10 kV impact of a  $\text{Cu}^+$  ion indicating a typical single-maximum curve. One can see that the shock waves generated at the impact were efficiently removed from the system by the system thermal boundaries.

Each sputtering yield value was repeated over  $\sim 100$  ion impacts. The average result shows that the error of the final average yield was less than 5%.

In order to simulate induced surface charges in high electric fields, the target copper atoms within a thin layer of one lattice parameter  $a_0$  were supplied electric charges, which were obtained from an external electric field  $E_m=1\text{GV/m}$ , according to the Gauss law:

$$\sigma = \varepsilon_0 E_m, \quad (5)$$

where  $\epsilon_0$  is the dielectric permittivity of vacuum and  $E_m$  is the magnitude of the surface electric field in the rf cavity. The total charge obtained by Eq. (5) was uniformly distributed among the surface layer atoms. Interactions between the surface charges were modeled via a Yukawa-type (screened Coulomb) potential with a Thomas-Fermi screening length  $a_{TF} = 3^{1/2} v_F/\omega_p$ , where  $v_F$  is the Fermi velocity and  $\omega_p$  is the plasma frequency [24].

## 2.2. Coulomb Explosion Models

Coulomb explosion (CE) is a well-known phenomenon in the area of swift, heavy, and highly charged ion collisions with targets [13,24,25]. To simulate Coulomb explosion, we chose several types of surface nanometer scale tips at high temperatures and applied strong electric field: (1) a blunt hemispherical bump (radius of the hemisphere was  $43\text{\AA}$ ) with a charge uniformly distributed on the surface of the bump; (2) a sharp copper tip (height of  $22\text{\AA}$ ) on a copper surface with the charge distributed in accordance with the local surface curvature; and (3) a cubic copper sample of  $50\times 50\times 50\text{\AA}^3$  in vacuum that was placed near the surface and charged by dark-current electrons in accordance with the surface shape (curved locations have larger charge density).

The total charge was obtained by using the Gauss law for the electric field obtained by the Vorpal package on the order of 1-10 GV/m. The Vorpal (average) surface electric field was multiplied by an enhancement factor  $\beta$  to take into account the shape of the protrusion. This parameter was discussed in detail in our previous papers [1,4].

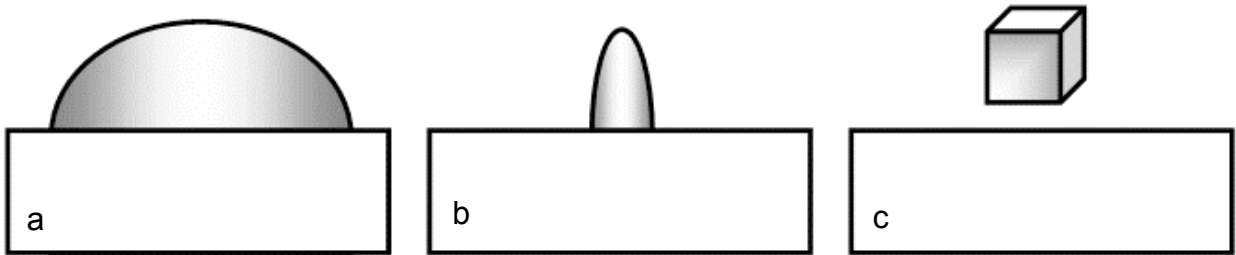


Fig. 3. Coulomb explosion simulation at  $T_s=300-800\text{K}$ : (a) blunt hemi-spherical bump uniformly charged on the surface; (b) sharp copper tip on copper surface charged according to its curvature; (c) cubic copper sample placed near the surface and charged by dark-current electrons in accordance with the surface shape (curved locations have larger charge density).

During CE simulation, the kinetic energies of the atoms belonging to the tip or bump were calculated, and an energy distribution function (EDF) was calculated at different time instants. This variable is a necessary boundary condition function that should be supplied to the Vorpal particle-in-cell simulation package developed by Tech-X in order to simulate plasma formation in rf structures.

## 3. Simulation Results

In this section we present our simulation results for sputtering yields and for Coulomb explosion.

### 3.1 Sputtering Yield at Room Temperature

MD simulations of the copper self-sputtering yields were performed at various temperatures (300, 800, and 1300K) and for a wide range of ion energies from 50 eV to 50 keV. The obtained calculated yields were compared with the existing experimental and simulation results [17-24], and this comparison is shown in Fig. 4.

In Fig. 4, our simulation results for two potentials are shown by blue symbols. The Cleri potential [29] results are close to the results obtained by MD simulation by Abrams et al. at oblique impact angles [22]; and they are higher than those obtained by using the Rosato potential [28]. These two potentials give close results at energies of 1 keV and above.

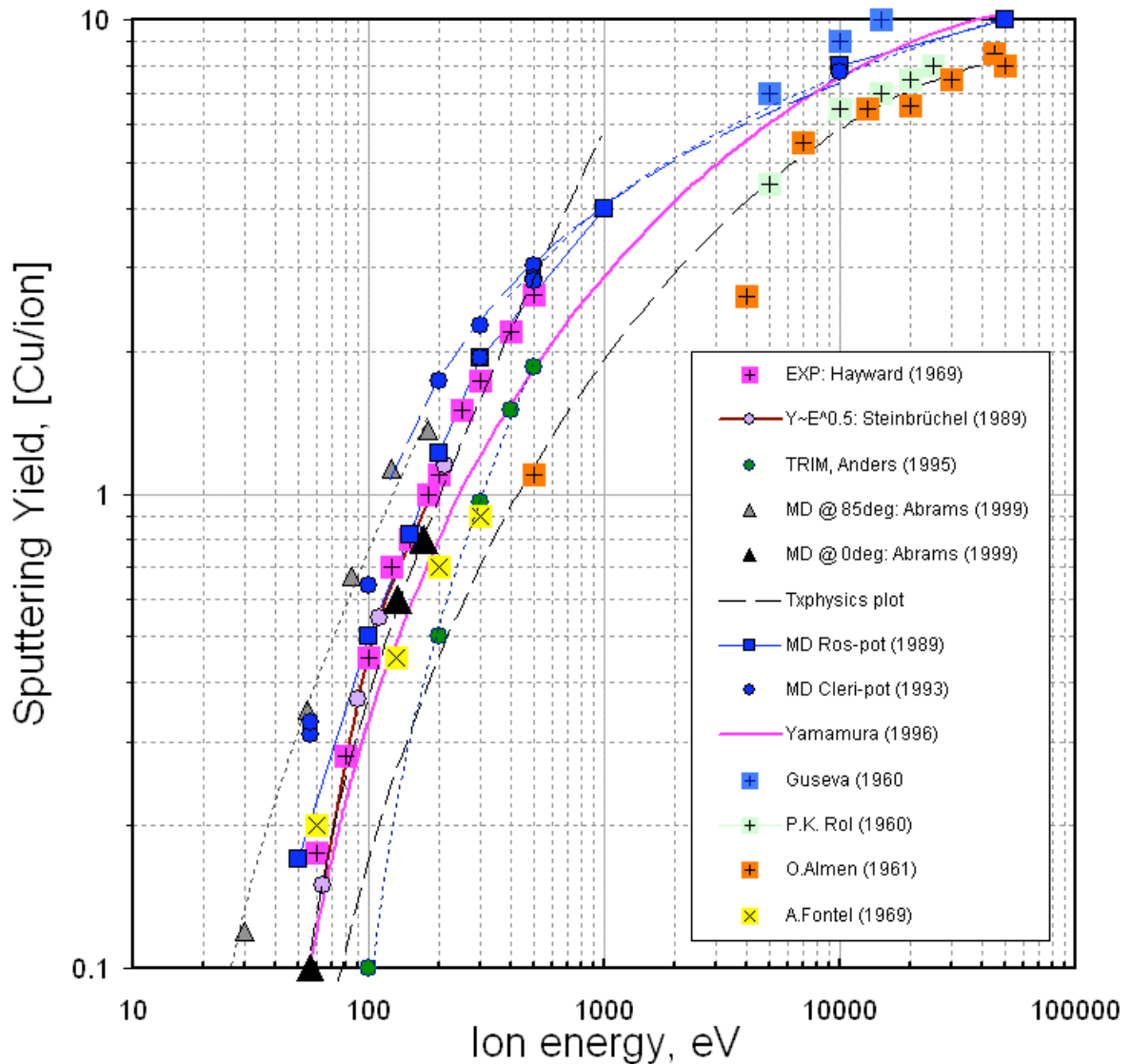


Fig. 4. Comparison of our MD simulation results for the copper self-sputtering yields with existing experimental and simulation results [17-23]. The pink line is the reference line given by the empirical model of Yamamura et al. [20]. The green circles are obtained by a Monte Carlo TRIM code [20,21] in a binary-collision approximation. The dashed line is a Txphysics (Tech-X Inc) approximation of the Yamamura's model. Color symbols with crosses are

experimental data given by Yamamura et al. [20]. Our MD calculation results for two EAM potentials developed in [28,29] are given by blue symbols. Black and gray triangles are the MD simulation results obtained for Cu<sup>+</sup> ion collisions of a Cu surface bombarding at 0° and 85° angles off the normal to the surface [22].

Monte Carlo T-DYN 4.0 and TRIM-Cascade 3.1 binary-collision approximation codes developed in [19] were used for sputtering yield simulation in [20,21]. The pink line is the reference line given by the empirical model of Yamamura et al. [20]. This model underestimates the sputtering yield by a factor of 1.7 at energies between 100 eV and 1 keV. The green circles are obtained by a Monte Carlo TRIM code [20,21] that uses a binary-collision approximation.

Our MD results show that TRIM underestimates the sputtering yield at 100 eV by a factor of 5 and twice that at an energy of 500 eV. TRIM gives results close to MD at energies above 50 keV. Figure 4 shows that the Monte Carlo data are much lower than experimental and MD data. This is a typical result showing that the binary-collision approximation cannot adequately describe the low-energy ion-target collisions. MD results were obtained at low and high energies and they are close to the experimental data. MD results shown as black solid triangles in Fig. 4 correspond to an oblique incident angle of 85° and gray triangles to normal ion incidence.

Experimental [16,17,20] and simulation papers [21,22] on self-sputtering of copper surfaces were analyzed, and the simulated sputtering yield data were compared to them. Sputtering yields of Cu<sup>+</sup> ions on polycrystalline copper films for energies below 1 keV were measured in situ by using crystal microbalance techniques in [16]. The yields varied almost linearly at energies above 50 eV (see Fig. 4). The experimental threshold energy for physical sputtering, approximately of 60 eV for the normal ion impact, was obtained from the work of Steinbrüchel [17].

The simulation results for copper self-sputtering were also arranged as a QuickTime movie that can be downloaded from the Argonne website ([sputter](#)).

### 3.2 Sputtering Yield at High Surface Temperatures

Although the mechanism of self-sputtering seems to be capable of fueling a low-density plasma studied in coating technology [9,10], there is no direct evidence that this mechanism is applicable to the dense plasma that can be generated in high-gradient linacs. One possible way to increase the sputtering yield is to heat the surface, thus efficiently reducing the surface binding energy due to thermal expansion of lattice.

The Fowler-Nordheim current is one of the possible sources of increasing the surface temperature. Our previous OOPIC simulations<sup>3</sup> showed that the copper surface becomes very hot within a few nanoseconds in a close vicinity of the plasma and can be melted. In this

---

<sup>3</sup> To be published elsewhere

section we present our MD results for simulation of the sputtering yield from a solid surface at 800K and from a liquid copper surface at melting temperature of 1310K.

A liquid Cu surface was prepared by heating a copper substrate to the melting temperature of 1310 K and equilibrating this configuration and storing it as an input file for the sputtering yield calculations. The lattice parameter and cut-off radii were adjusted to accommodate high-temperature expansion according to Eq. (4). The ion energies were selected between 50 and 150 eV, which corresponds to the sheath potential value obtained by our OOPIC simulation. Approximately 100 ion impacts at each ion energy were simulated. The results, given in Fig. 5, show that the plasma can get a significant flux from the liquid surface.

The most important result is the self-sputtering yield at 800K for an ion energy of 100 eV, which was obtained to be approximately 2.5, well below the melting point at 1310K. This means that the mechanism of self-sputtering is self-sustained for the unipolar arc plasma in *rf* linacs. The main reason is the high plasma density,  $\sim 10^{25} \text{ m}^{-3}$ , which creates a relatively high sheath potential and thus enables heating the surface by electron current.

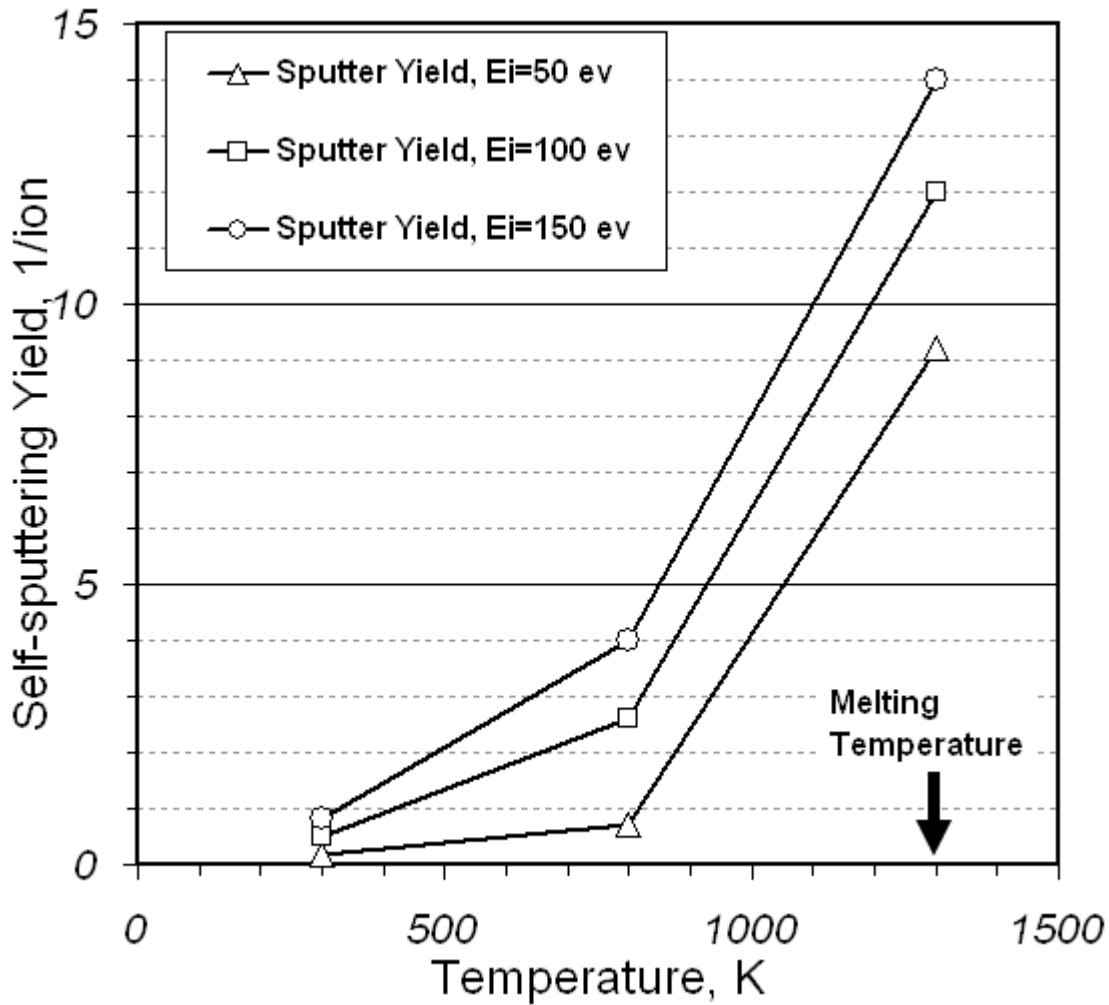


Fig. 5. Sputtering yield of a 50-150 eV Cu<sup>+</sup> ion on a copper surface at T=800K.

### 3.3 Sputtering Yield of a Uniformly Charged Surface

The electric field affects the surface self-sputtering in two ways. One way is that the field accelerates the bombarding ion up to 100-150 eV, according to our OOPIC simulations. The second way is that a high electric field brings electric charges to the cavity surface, thus making surface atoms less cohesive; and in principle this effect should increase erosion. In order to understand the efficiency of *rf* cavity copper surface self-sputtering by this mechanism, surface charges induced by a high surface electric field were uniformly distributed in the thin top layer of the target copper atoms.

Figure 6 shows the results of our MD simulations of self-sputtering of copper *rf*-cavity surface by accelerated  $\text{Cu}^+$  ions, at an ion energy of 100 eV and a surface temperature of 800K.

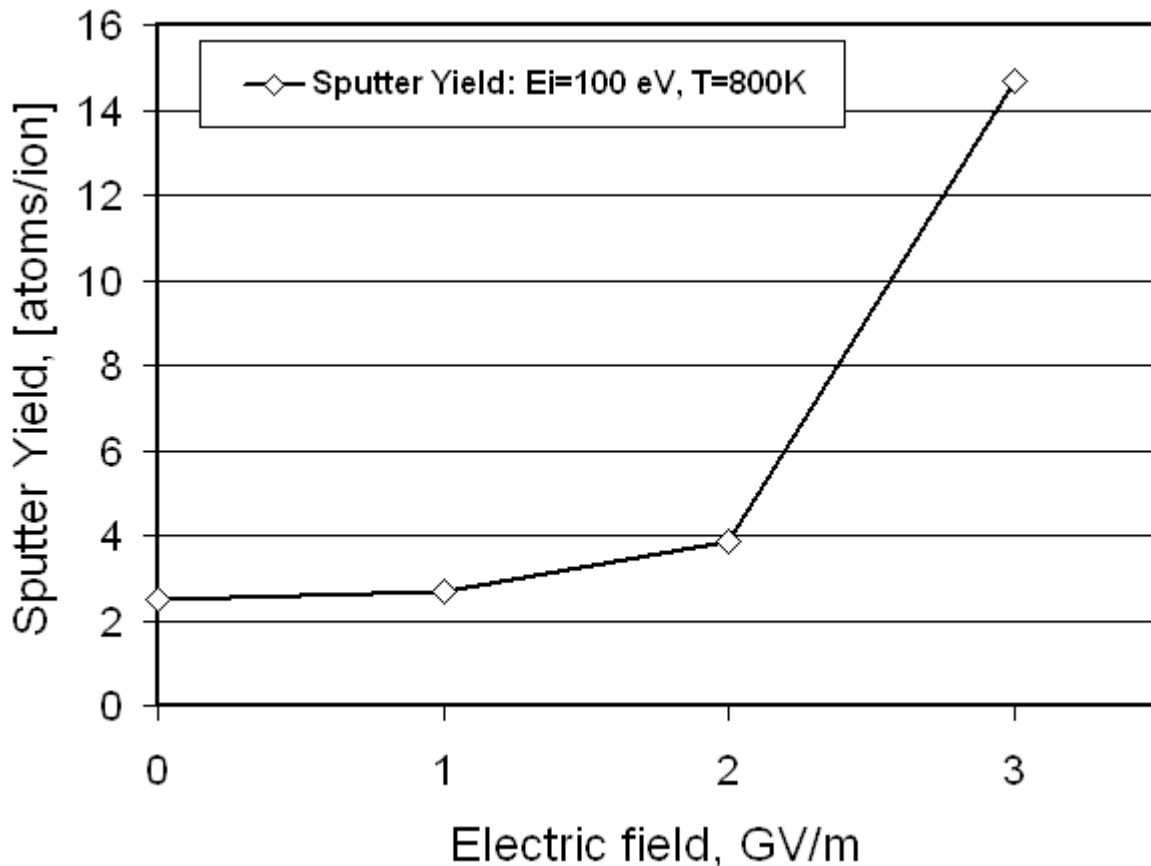


Fig. 6. Dependence of the copper self-sputtering yields on the strength of electric field (not on ion energy – see remark at the beginning of this section) calculated by MD at a surface temperature of 800K and an ion energy of 100 eV.

The results show that both high temperature and high electric field can significantly increase the surface erosion. Both mechanisms will be important in a real *rf* cavity. We believe that the unipolar arc model explains the mechanism of *rf* breakdown by attracting the mechanism of self-sputtering of hot copper surface residing at a very high local electric field (depending on

the local curvature). This mechanism has never been addressed before in *rf* breakdown studies. The main reason for overlooking the self-sputtering mechanism was the fact that the yield at such low energies is normally less than unity, which immediately removes this mechanism from consideration as being viable. However, our simulation has showed—for the first time—that surface temperature and surface local field can significantly increase the erosion yield by a factor  $> 10$ .

We note that the earliest unipolar arc model for Tokamak studies was developed based on an arbitrary assumption that the surface erosion rate was  $\sim 10$  [11,12]. Here we confirm such high erosion rates at the *rf* cavity surfaces.

### 3.4 Coulomb Explosion Simulation Results

Our previous simulations did not take into account screened Coulomb interaction between various parts of the charged tip. Therefore, they did not include a mechanism where the charged tip can explode while sitting on the top of the surface. Our new (preliminary) results show clearly (see Fig. 7) that the nanoscale tip can explode into vacuum while being on the surface. Therefore in principle these results can be used to verify the mechanism of baking of the tips.

Energy distribution functions are presented in Fig. 8.

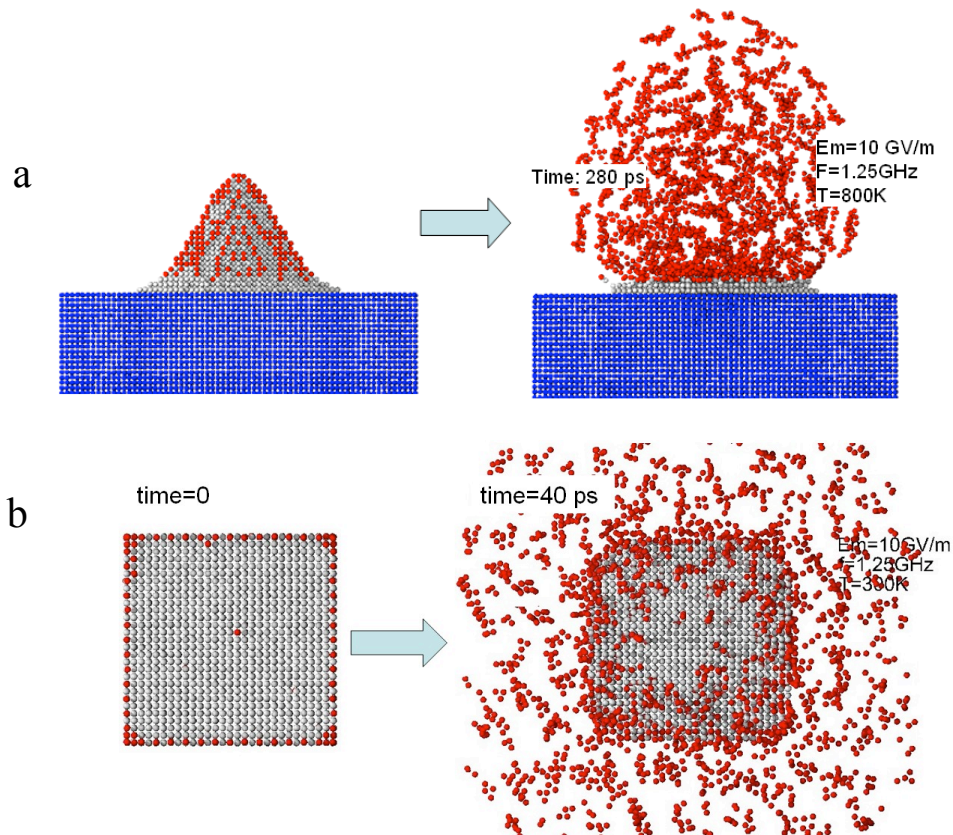


Fig. 7. Coulomb explosion of a conical tip placed on the surface: (a) simulation with an electric field of 10 GV/m and an  $rf$  frequency of 1.25 GHz, at room temperature; (b) simulation of a cubic copper sample Coulomb explosion by our MD simulation. Right figures show the results of shock-wave expansion at a time instant of (a) 280 ps and (b) 40 ps after the beginning of the Coulomb explosion.

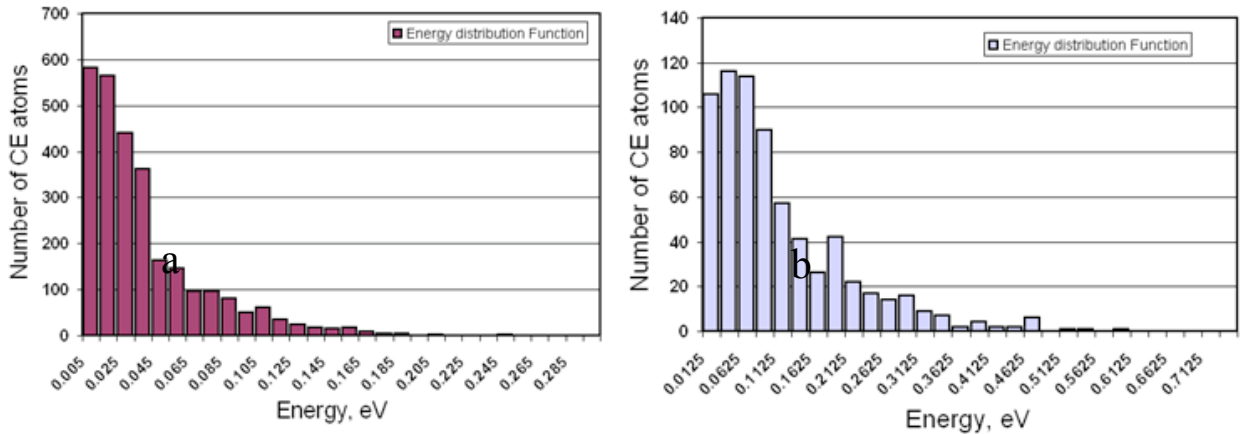


Fig. 8. Energy distribution function for the Coulomb explosions: (a) for a tip placed on the cavity surface, with an electric field of 10 GV/m and an  $rf$  frequency of 1.25 GHz, at 800K; (b) EDF of a cubic copper fragment placed in vacuum, then charged and exploded by Coulomb explosion.

### 3.5. Simulation Results for Taylor Cone Development

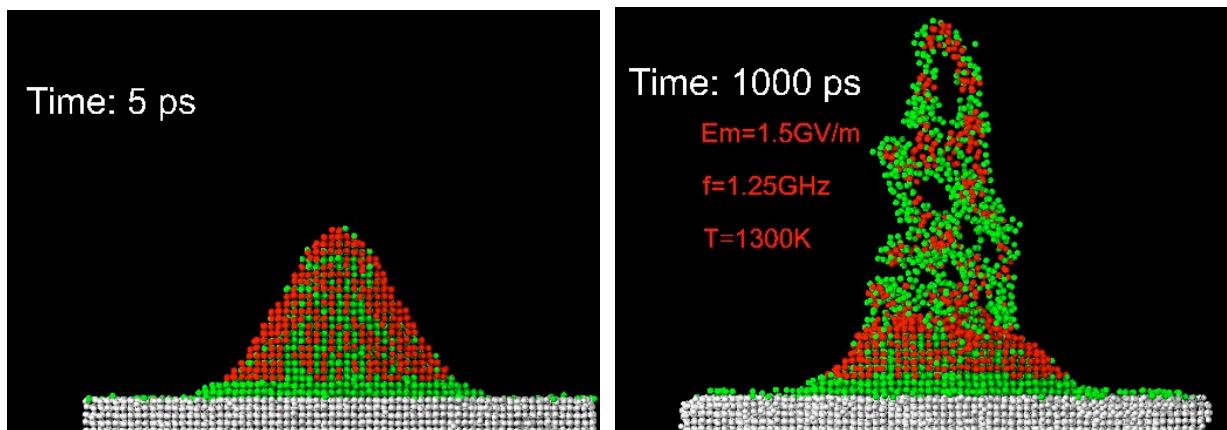


Fig. 9. Taylor cone simulation was conducted at 300, 800, and 1300 K to understand the effect of the surface temperature on the tip's shape in strong electric field.

Taylor cone development was simulated because we believe this is one of the major mechanisms for surface Coulomb explosion. Our simulations were conducted at 300, 800, and 1300 K, which is slightly below the melting temperature. A small, cone-shaped tip sample is shown in Fig. 9, and a large simulation dome-shaped tip is shown in Fig. 10.

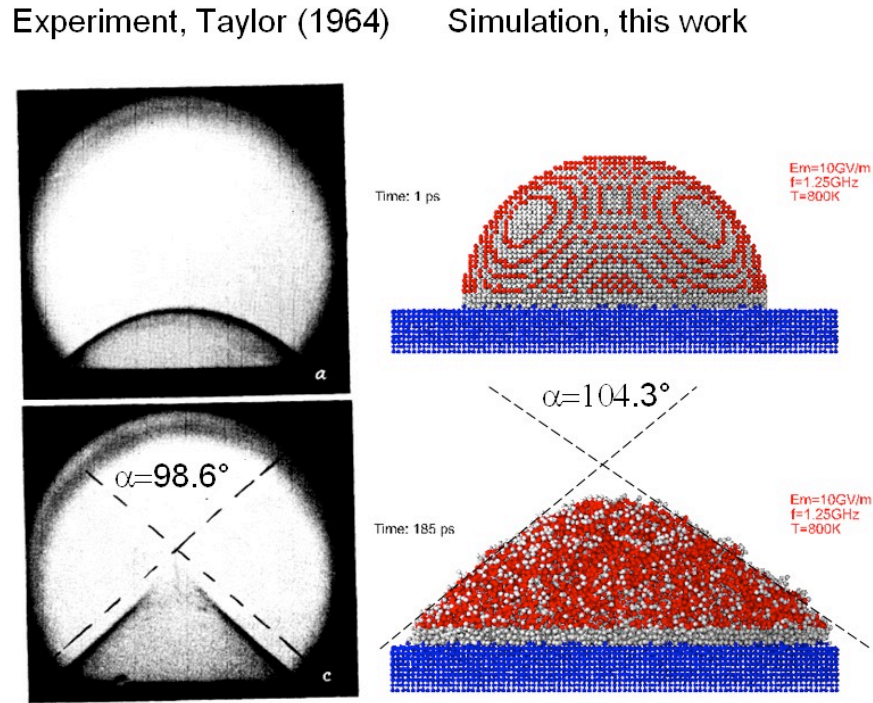


Fig. 10. Taylor-cone simulation for a hemispherical tip shape at 1300 K in a strong electric field of 10 GV/m. We found that the Taylor cone was formed after a 185 ps simulation that has 104.3° (two right color figures). This simulation result is comparable to the experimental result of Taylor, 98.6° [30], which is shown in the two left (black-and-white) figures. This is the first simulation of Taylor cone development on an *rf* cavity surface.

The simulation results were also presented as QuickTime movies that can be downloaded from the Argonne website ([weak Coulomb explosion](#), [large Coulomb explosion](#)).

#### 4. Unipolar Arc Formation Mechanisms

In order to understand the fluxes emitting from the copper surface and therefore fueling the plasma in *rf* cavity, various electron and ion currents and neutral atomic fluxes were schematically plotted in Fig. 11.

Plasma is initiated by the accumulative actions of electron heating and surface erosion via a high electric field gradient. As we showed previously, field evaporation of small chunks of surface protrusions, tip, foreign atoms, and oxide layers that enhance the electric field

gradient can start as early as at 7 GV/m [4]. Surface will be heated via Fowler-Nordheim, Child-Langmuir, thermionic, Bohm currents, and  $\text{Cu}^+$  ion flux from plasma.

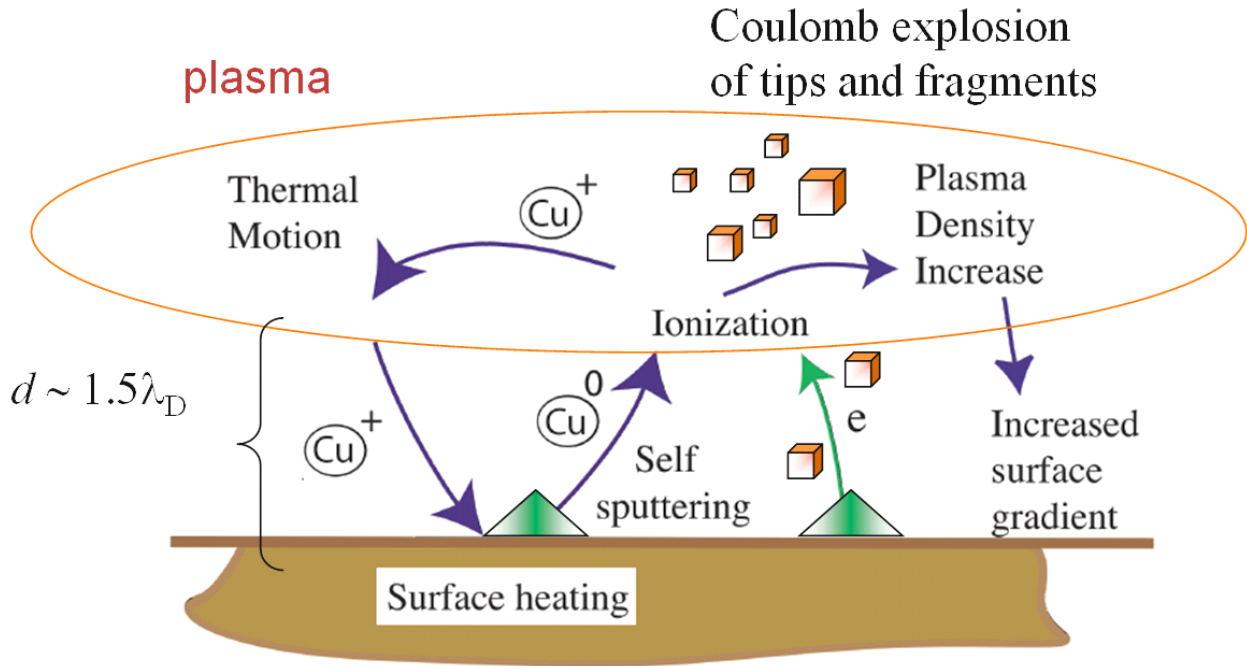


Fig. 11. Schematic of the near-surface processes and fluxes from and to plasma (see explanations for the fluxes in the text).

This understanding is based on a unipolar arc model developed in [11,12] for Tokamak first wall erosion by plasma to understand the *rf* cavity high-gradient breakdown. The importance of self-sputtering for self-sustained plasma discharge was first emphasized in [9,10], where a low-density plasma was considered.

Our concept of unipolar arc in *rf* cavities is based on the following basic elements: (1) *rf* cavity plasma can have much higher density of about  $\sim 10^{25} \text{ cm}^{-3}$ <sup>4</sup>; (2) as a consequence, the Debye length is much smaller—our estimates show it is on the order of a few nanometers; (3) the sheath thickness is much lower than that for coating technology [9,10]; and (4) the electric field is much stronger—estimates give the values from 1 to 10 GV/m at the above plasma density.

Therefore, we extended the unipolar arc model by switching to a high-density plasma and we added plasma simulations with OOPIC and atomistic simulations of self-sputtering yield into this model. As a result, the unipolar arc model in principle can explain all the effects and processes occurring in the near-surface space for time intervals from picoseconds to almost 10 nanoseconds.

<sup>4</sup> According to our OOPIC simulations – to be published elsewhere

To understand the fluxes emitting from the copper surface and fueling the plasma in the *rf* cavity, various electron and ion currents and neutral atomic fluxes were compared (see Fig. 12): (1) the Fowler-Nordheim current for electrons, (2) the Child-Langmuir ion current from plasma to the tip, (3) the Richardson-Dushman thermal emission of electrons from the tip, and (4) the sputtering flux obtained via the Bohm current (plasma fluxes) multiplied by the MD sputtering coefficient .

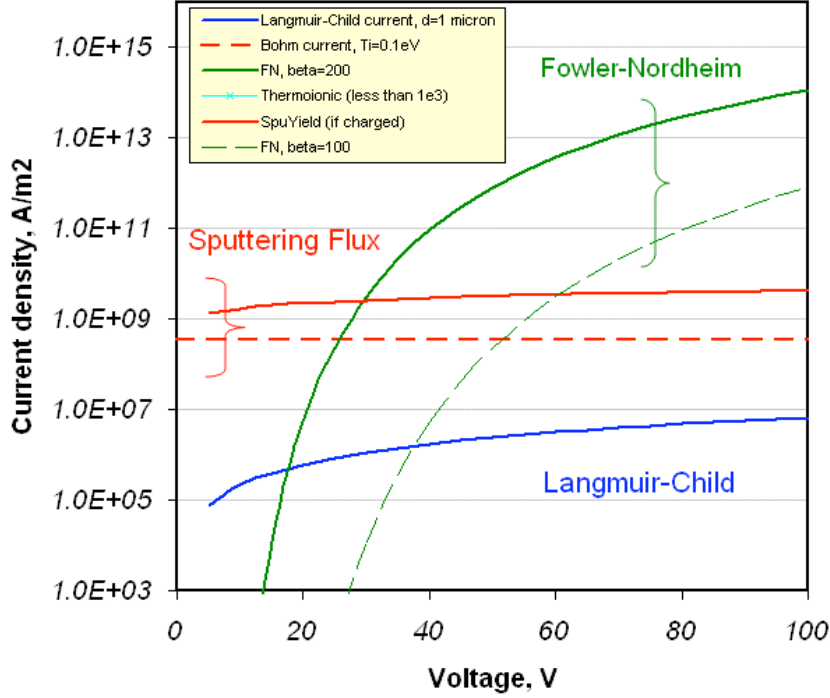


Fig. 12. Comparison of different mechanisms of electron emission with the sputtering flux. The following curves are shown: (1) Fowler-Nordheim current (green line) for two enhancement factors ( $\beta = 100$  – dashed line,  $200$  – solid line); (2) Langmuir-Child equation for ion current from plasma to the tip ( $d=1$  mm); (3) Richardson-Dushman equation for thermionic emission of electrons from liquid Cu ( $T=1300\text{K}$ ); (4) sputtering flux, calculated from Bohm current (plasma ion fluxes) times the sputtering yield at  $1300\text{K}$ .

The total current density consists of three major components:

$$j_{\Sigma} = j_{FN}^- + j_{Child}^+ + j_{therm}^- ,$$

$$j_{FN}^- = \left[ 1.541 \times 10^{-6} \frac{E^2}{\varphi} t^2(y) \right] \times \exp \left[ - 6.831 \times 10^7 \left( \frac{\phi^{3/2}}{E} \right) v(y) \right], A/cm^2 \quad (6)$$

where  $E = \beta E_0$

$$j_{Child}^+ = \frac{4\epsilon_0}{9} \sqrt{\frac{2e}{m_i}} \frac{V^{3/2}}{d^2}, \quad (7)$$

$$j_{therm}^- = \lambda A_0 T^2 \exp \left[ - \frac{e\phi}{k_B T} \right], \quad (8)$$

$$\rho c_v \frac{\partial T}{\partial t} = j^2 \delta + \nabla(k \nabla T), \quad (9)$$

Our comparison in Fig. 12 clearly shows that the main mechanism at low plasma sheath potentials (less than 50-100 eV) is the self-sputtering mechanism. This fact confirms our new unipolar arc model of high-gradient breakdown in warm *rf* linacs (to be published elsewhere).

## 5. Summary

Experimental and simulation papers on self-sputtering of Copper surfaces were analyzed and the existing sputtering yield data were preliminarily compared. A molecular dynamics (MD) code was developed to calculate the Cu+/Cu self-sputtering yields at different substrate temperatures and in a wide range of ion energies between 50 eV and 50 keV.

Sputtering yields were calculated from charged copper surfaces, where the charges were induced by high local electric fields (1 and 10 GV/m), as suggested by our OOPIC plasma simulations. Our results clearly show that the erosion rate of the copper self-sputtering mechanism can be significantly large ( $Y > 10$ ). This fact makes the self-sputtering of hot and charged copper cavity surface the main mechanism of erosion and crater formation and provides insight into the high-gradient *rf* breakdown phenomenon.

A Coulomb explosion of two types of surface protrusions and a charged cubic sample placed close to the surface in plasma also were simulated by MD, and energy distributions were obtained. The atomic fluxes and energy distributions were used as input for coupling MD with a continuum Vorpil plasma simulation code developed by Tech-X. A Taylor cone formation was obtained by our MD simulation after the system was evolved over 185 ps. The MD Taylor cone has an apex angle of 104.3°, which is close to the experimental value of 98.6°. This is the first simulation of Taylor cone development on an *rf* cavity surface.

## Acknowledgments

This work was supported in part by the U.S. Dept. of Energy under Contract DE-AC02-06CH11357 and in part by SBIR with Tech-X Corp.

## References:

- [1] A. Hassanein, Z. Insepov, J. Norem, A. Moretti, Z. Qian, A. Bross, Y. Rorun, R. Rimmer, D. Li, M. Zisman, D.N. Seidman, K.E. Yoon, Effects of surface damage on rf cavity operation, *Phys. Rev. STAB* 9 (2006) 062001.
- [2] J. Norem, V. Wu, A. Moretti, M. Popovic, Z. Qian, L. Ducas, Y. Torun, N. Solomey, Dark current, breakdown, and magnetic field effects in a multicell, 805 MHz cavity, *Phys. Rev. ST Accel. Beams* 6 (2003) 072001.
- [3] J. Norem, Z. Insepov, I. Konkashbaev, Triggers for rf breakdown, *Nucl. Instrum. Methods Phys. Res., Sect. A* 537 (2005) 510.
- [4] Z. Insepov, J.H. Norem, A. Hassanein, New mechanism of cluster-field evaporation in rf breakdown, *Phys. Rev. ST Accel. Beams* 7, 122001 (2004).
- [5] Feasibility Study-II of a Muon Based Neutrino Source, edited by S. Ozaki, R. Palmer, M. Zisman, and J. Gallardo, BNL-52623 (2001), <http://www.cap.bnl.gov/mumu/studyii/>
- [6] M.M. Alsharo'a et al., Recent progress in neutrino factory and muon collider research within the Muon Collaboration, *Phys. Rev. ST Accel. Beams* 6 (2003) 081001.
- [7] <http://www.linearcollider.org/cms/>
- [8] <http://www.slac.stanford.edu/grp/ara/HGCollab/HomePage/HGhome.htm>
- [9] A. Anders, S. Anders, M.A. Gundersen, Electron emission from pseudospark cathodes, *J. Appl. Phys.* 76 (1994) 1494-1502.
- [10] A. Anders, *Cathodic Arcs: From Fractal Spots to Energetic Condensation*, Springer Series on Atomic, Optical, and Plasma Physics, Springer (2008).
- [11] F.R. Schwirzke, Vacuum breakdown on metal surfaces, *IEEE Trans. on Plasma Sci.*, 19 (1991) 690-696.
- [12] F.R. Schwirzke, X.K. Maruyama, Onset of breakdown and formation of cathode spot, *IEEE Trans. on Plasma Sci.*, 21 (1993) 410-415.
- [13] Z. Insepov, M. Terasawa, K. Takayama, Surface erosion and modification by highly charged ions, *Phys. Rev. A* 77, 062901 (2008).
- [14] R.L. Fleischer, P.B. Price, R.M. Walker, E.L. Hubbard, Criterion for Registration in Dielectric Track Detectors, *Phys. Rev.* 156, (1967) 353-355.
- [15] A. Ootuka, K. Kawatsura, F. Fujimoto, K. Komaki, K. Ozawa, M. Terasawa, Single and Double K-Shell Ionization Cross Sections of Beryllium by C, N, O and Ne Ion Bombardments, *J. Phys. Soc. Jpn.* 53, 1001 (1984).
- [16] W.H. Hayward, A.R. Wolter, Sputtering yield measurements with low-energy metal ion beams *J. Appl. Phys.* 40 (1969) 2911.
- [17] C. Steinbrüchel, Universal energy dependence of physical and ion-enhanced chemical etch yields at low ion energy, *Appl. Phys. Lett.* 55, (1989) 1960.
- [18] H.M. Urbassek, Molecular-dynamics simulation of sputtering, *Nucl. Instr. Meth. in Phys. Res. B* 122 (1997) 427-441.
- [19] J.P. Biersack et al, T-DYN Monte Carlo simulations applied to ion assisted thin film processes, *Nucl. Instrum. Meth. B* 59/60 (1991) 21-27.
- [20] Y. Yamamura, H. Tawara, *Atomic Data and Nuclear Data Tables* 62 (1996) 149-253.
- [21] A. Anders, M.A. Gundersen, Self-sustained self-sputtering: a possible mechanism for the superdense glow phase of a pseudospark, *IEEE Trans. Plasma Sci.* 23 (1995) 275-282.
- [22] C.F. Abrams, D.B. Graves, Cu sputtering and deposition by off-normal, near-threshold  $\text{Cu}^+$  bombardment: Molecular dynamics simulations, *J. Appl. Phys.* 86 (1999) 2263-2267.

- [23] H. Gades, H.M. Urbassek, Energy deposition, reflection and sputtering in hyperthermal rare-gas→Cu bombardment, *Appl. Phys. A* 61 (1995) 39-43.
- [24] E.M. Bringa, R.E. Johnson, Coulomb explosion and thermal spikes, *Phys. Rev. Lett.* 88 (2002) 165501.
- [25] R.L. Fleischer, P.B. Price, R.M. Walker, Ion explosion spike mechanism for formation of charged-particle tracks in solids, *J. Appl. Phys.* 36 (1965) 3645-3652.
- [26] Z. Insepov, R. Manory, J. Matsuo, I. Yamada, Proposal for a hardness measurement technique without indenter by gas-cluster-beam bombardment, *Phys. Rev.* 61 (2000) 8744-8752.
- [27] Z. Insepov, I. Yamada, M. Sosnowski, Sputtering and smoothing of metal surface with energetic gas cluster beams, *Mater. Chem. Phys.* 54 (1998) 234-237.
- [28] V. Rosato, M. Guillope, B. Legrand, Thermodynamical and structural properties of f.c.c. transition metals using a simple tight-binding model, *Philos. Mag. A* 59 (1989) 321.
- [29] F. Cleri, V. Rosato, Tight-binding potentials for transition metals and alloys, *Phys. Rev. B* 48 (1993) 22.
- [30] G. Taylor, Disintegration of water drops in an electric field, *Proc. R. Soc. Lond. A* 280 (1964) 383-397.

The submitted manuscript has been created by UChicago Argonne, LLC, Operator of Argonne National Laboratory ("Argonne"). Argonne, a U.S. Department of Energy Office of Science laboratory, is operated under Contract No. DE-AC02-06CH11357. The U.S. Government retains for itself, and others acting on its behalf, a paid-up nonexclusive, irrevocable worldwide license in said article to reproduce, prepare derivative works, distribute copies to the public, and perform publicly and display publicly, by or on behalf of the Government.